Journal of International Scientific Publications: Materials, Methods and Technologies

Volume 8, ISSN 1314-7269 (Online), Published at: http://www.scientific-publications.net

COMPLEX ANALYSIS OF THE STATE OF THE WALL CONCRETE OF "BELI ISKAR" DAM AFTER 70 YEARS OF EXPLOITATION

Valeriy Borisov Naydenov

Institute of Mechanics - Bulgarian Academy of Sciences

1113 Sofia, Acad. G. Bonchev Street, Block 4

Abstract

The massive gravity wall of the "Beli Iskar" dam was constructed as a high-mountain hydro-technical facility in the period 1939-1945. It is 1900 m above the sea level and is part of the system of water supply of the city of Sofia. The wall bars the valley of the Beli Iskar river, and its length is 570 m, maximal height - 40 m, and dam live volume - about 15 millions m^3. The wall was built of non-reinforced concrete and its approximate volume is over 220 000 m^3, while separate wall sections were revetted with granite blocks. Dam durable exploitation accompanied by the intensive action of inflowing soft waters, as well as that of environmental factors, resulted in serious concrete corrosion.

The report presents a synthesized analysis of the basic results of various inspections - technical, visual, destructive and non-destructive tests, complex structural analysis identifying potential corrosion development and its impact on the products of hydration, technical evaluation of the state of the wall concrete. Basic conclusions are drawn and specific recommendations to facility future exploitation are made.

Key words: *concrete, destructive and non-destructive tests, strength-deformation characteristics, complex structural analysis*

1. TECHNICAL INSPECTION AND VISUAL OBSERVATION IN ASSESSING THE ACTUAL STATE OF THE WALL CONCRETE

1.1 Preliminary data

Limited evidence on concrete prescribed composition was found. Yet, three basic recipes of concrete preparation were used in the past, involving various portions of ordinary Portland cement produced by "Granitoid"– the only local cement plant operating at that time. Those three types of concrete were packing concrete with cement contents of 280 kg/m^3, concrete used to cast the wall bulk (including the wall facade, i.e. the wall "air" side (wall/air interface)) with 185 kg/m^3 cement contents and concrete used in casting the wall tooth with 300 kg/m^3 cement contents. Compressive strength of the used cement of standard age (28 days) was found as exceeding 550 kg/cm^2. Hence, it seemed that cement strength was high, but the material would display high exothermy. This could affect concrete quality during cast of massive single volumes.

The coarse aggregates were in the form of pieces of broken local granite. Aggregates with different grain size were used in specific concrete recipes – 100 mm (for packing and basic concrete) and 30 mm (for the wall tooth). Records proved that the grain size of the river sand used was 0-7 mm. No data for the water/cement ratio were available.

That evidence predetermined the characteristics of the concrete mix and most of all, the necessity to undertake special measures to attain maximal aggregate packing and thus- maximal compaction of the cast concrete section. Obviously, no chemical or mineral admixtures were added. No record on the processing of the work joints was found. Joints were vertical (between the separate blocks) and horizontal (within one and the same block and distributed along the block height).

A previous expertise treating the state of the basic concrete of the dam wall provided data on the variation of concrete compressive strength in time. It was assumed that the compressive strength of concrete of standard age amounted to about 21,50 MPa during wall construction. It logically increased to 37,50 MPa after 5 years of dam exploitation. Then, owing to corrosion and soft water filtration, it gradually decreased to 21,90 MPa after a period of 42 years and subsequently - to 15,40 MPa after a period of 59 years.

Records on successive repairs were found - fabrication of packing curtains strengthening the wall bulk, various processing of joints, assembling of a geo-membrane on the wall "water" side (the wall/water interface). Yet, the technical effect of those measures was limited.

1.2 Spread of the technical control

The technical control and the visual inspection were performed at easy-to-access spots – mainly at the "air" side of the wall and in the technical premises and gallery. Identification of the segments (blocks) of the dam wall was made during the inspection. It was established that monolithic casting of those wall components was performed, separating them by vertical work joints. We undertook specific actions in the course of the study: visual inspection and identification of the state of each segment and that of the joints (horizontal and vertical) within and between them; identification of visual defects; detection, localization and identification of the type of cracks having occurred on separate blocks and within areas with non-coated and/or unprotected reinforcement (where available); identification of the state of the reinforcing steel, identification of the visual modification of the concrete structure due to atmospheric, exploitation, corrosion or other impacts; identification of the visual active leakage or leakage traces located in different wall sectors.

Those actions agreed with the world practice of inspection of large dam walls – ***ICOLD (2008)*** and International Commission on Large Dams, ***Bulletin 136 (2009).***

1.3 Results of the technical control

The performed technical control yielded the following major conclusions:

The object of investigation is an impressive hydro-technical facility, considering the period of dam construction and the then-available technological capabilities, together with the object hard accessibility and high-mountain location. The wall is 40 m high at its central section, its total length is about 570 m, and the approximate width of the wall central section amounts to 30 m. Granite revetment covers the entire wall at the side of the dam cup (the wall/water interface). Most of its part is invisible due to the deposition of a PVC geo-membrane. A paved road is built along the wall upper edge (3,4–3,5 m thick). Technical premises are erected in the middle (at the wall air side), where valves of the dam discharge pipelines are mounted. Premise walls are built of concrete and stone, while the roof is a steel reinforced slab.

The wall is segmented into sections (blocks) along its length, and blocks are concreted independently. Work joints are shaped within and between the blocks. The fresh concrete has been prepared on the spot and fed to the construction site: (i) horizontally- by trams rolling on rails and (ii) vertically-through pipes supplied with feeding funnels (bunkers). The method of concrete mix compaction is unknown –it seems to have been some type of rolling. Wood casing has been used- its traces are seen on the wall air side.

The vertical cast of the concrete mix was not continuous, which resulted in the formation of technological voids (due to casting on hardened concrete). Those voids violated the structure solidity and their occurrence turned to be a weak point, since they permitted water filtration through the wall cross section. Besides, the violated solidity favored the formation of potential slip planes when applying mechanical impacts, thus compromising the seismic stability of the entire structure.

Obviously, concrete mix compaction was non-uniform and insufficient, which yielded non-homogeneity of the concrete massive, i.e. formation of areas of non-compacted concrete, concrete stratification, formation of loose gravel surface and occurrence of large air pores and voids. The concentration of those defects was significant in the areas around the technological joints and along the boundaries between the wall sections.

Concrete of the wall air side still undergoes direct atmospheric impacts – solar radiation, cyclic wetting and drying, freezing and unfreezing. Variable wetting and drying originate cyclic stresses, which act as fatigue stresses and gradually compromise the material structure. Ice destructive impacts are well known and described in literature. They result in concrete gradual fracture, i.e. material caving and cracking, and the process runs more intensively in time, being directed outside- inside.

Besides atmospheric waters, filtration waters are also available in the areas around the technological joints and at the boundaries between separate wall sections. Regarding concrete violated density and structure, those are the sites where most serious material damage is expected to occur. It consists in the formation of large concrete caves, pores, caverns and voids.

Active and consolidated leaks are localized at a number of sites on the wall surface where free lime has been extracted from concrete. It is a product of hydration of basic clinker minerals-alite **(C_3S)** and belite **(C_2S)**.

Carbonized precipitants of the extracted lime are several centimeters thick at some spots. The process is known as concrete physical corrosion.

Yet, the carbonization effect is insignificant if water containing dissolved carbon dioxide is present. When calcium hydroxide dissolves and is extracted from concrete, concrete porosity increases, medium alkalescence decreases, and the stability of calcium hydro-silicates and hydro-aluminates produced by cement hydration is violated. Hence, concrete strength may drop by 50%. Yet, the plausibility of that hypothesis is still to be proved.

Leakage traces are also observed along some work joints separating the wall sections. Some of them have been additionally compacted. Increase of the width of the work joints in vertical direction (directed to the wall crown) is registered in most cases.

A premise housing the dam discharge valves is located in the wall middle area. Its roof plate is fabricated from cross-steel-fiber-reinforced concrete and consists of two layers. Hydro-insulation is deposited on the plate outside surface, and it is totally compromised. Plate concrete is seriously damaged by atmospheric impacts and water penetration. Reinforcement corrosion has advanced, and a thick layer of corrosion products (rust) covers the reinforcement.

A gallery is built inside the wall. Leaks are observed all over the walls and the vaulted roof, causing extraction of free lime. Lime precipitants, probably partially or totally carbonized, coat the gallery floor, walls and roof.

Moss covers the wall longitudinally and close to the ground, additionally arresting moisture. Thus, water freezes under temperature drop causing damage of concrete surface layer. As known, plants release acids, which are aggressive to the cement stone.

1.4 Visual inspection of the state of the concrete surface layer

The technical control provides a basis for: preliminary estimation of the state of the surface concrete; identification of corrosion damage; estimation of the potential of the surface concrete to protect the steel reinforcement (in the technical premises).

The availability of visual traces of extracted calcium hydroxide $\mathbf{Ca(OH)_2}$ in a number of areas of the wall air side, in the gallery and in the technical premises, as well as the visible corrosion of the steel reinforcement, plausibly proves concrete surface and in-depth damage. This implies the conduction of respective purposeful studies.

2. DESTRUCTIVE AND NON-DESTRUCTIVE STUDIES FOR THE IDENTIFICATION OF THE ACTUAL STATE OF CONCRETE AND REINFORCEMENT

2.1 Concrete compressive strength found via nondestructive testing

The probable compressive strength is found via non-destructive testing based on a correlation between concrete compressive strength and its surface hardness. Surface hardness is measured applying the so called method of elastic recoil (Shore method) using a sclerometer type “Schmidt N” in conformity with standard BDS EN 13791:2007 “On-site assessment of the strength of concrete in structures and ready-made elements”, BDS БДС EN 13791:2007/NA:2011 “On-site assessment of the compression strength of concrete in structures and ready-made elements. Nation-wide application (NA)” and BDS EN 12504-2:2012 “Testing of concrete in structures. Part 2: Non-destructive testing. Finding the recoil magnitude”.

Statistical processing of data is performed conforming to standard BDS EN 13791:2007/NA:2011 and BDS EN 206-1:2002 +A1/2006 + A2/2006 + HA:2008 “Concrete. Part 1: Specification, properties, preparation and correspondence + Nation-wide application (NA) of BDS EN 206-1:2002”.Control areas are selected (at least 3 points per each wall block), and the results of data statistical processing are shown in **Table 1.**

Table 1 Concrete data

Statistical characteristics	Value
Confidence interval –limits, N/mm^2	13,50 – 58,50
Arithmetic mean of concrete strength, N/mm^2	36,80
Standard deviation, N/mm^2	7,51
Variation coefficient	0,21
Characteristic strength of concrete, N/mm^2	23,70
Probable concrete class with respect to compressive strength	C 15/20 (B20)

The tested concrete corresponds to class C15/20 **(**B20), with respect to compressive strength, conforming to the classification specified by standard BDS EN 206-1/NA:2008. The found value of the variation coefficient of concrete compressive strength is larger than the normal one belonging to the interval 0,12-0,15. It shows the level of the technological discipline of casting (the accuracy of material dosing, uniformity of concrete mix compaction etc.) and the variation of material properties.

Since recoil test should be carried out on solid surface areas, it is not possible to correctly compare the probable compressive strength of the individual blocks. Moreover, since the arithmetic mean of strength is large (typical for concrete class C25/30, B30), the probable concrete class can be specified as **C 15/20** (**B20)** due to the large scatter of data.

2.2 Concrete compressive strength found by testing cores extracted from the structure

Cores are bored from the structure with a core boring machine. Samples are subsequently shaped into cylinders using a cutting disk. The direction of core shaping is perpendicular to the core axis.

The cylindrical samples are weighted with accuracy of 1 g. They are used to calculate concrete volumetric density and establish its non-homogeneity and the eventual availability of non-compacted areas. Loading surfaces are ground or coated conforming to the requirements of standard ISO 3310-1. Correction coefficients for core dimensions are chosen using Table NA.4 of standard BDS EN 206-1/NA.

The mean value of the volumetric density amounts to 2267 kg/m^3.

Results of core testing are statistically processed and given in **Table 2.**

Table 2 Statistical characteristics of the cores tested

Statistical characteristics	Value
Confidence interval-limits, N/mm^2	23,20 – 49,30
Arithmetic mean of concrete strength, N/mm^2	36,30
Standard deviation, N/mm^2	4,20
Coefficient of variation	0,12
Characteristic strength of concrete, N/mm^2	29,10
Probable concrete class with respect to compressive strength	C20/25 (B25)

Due to the tentative coring depth (about 50 cm), the strength found as typical for concrete of B25 class is higher than that found via nondestructive testing where it is correlated to concrete surface hardness. In this case, the effect of the strong corrosion of the recoil surface has been eliminated to a large extent.

A larger density of single results is observed, which directly affects the decreased coefficient of variation. The calculated coefficient is within relatively normal limits for concrete class C20/25 (B25)**.** Since cores were extracted from visibly solid areas of the concrete surface, correct comparison between values of compression strength found for separate blocks could not be made.

Taking as plausible the archive data on the strength of 5 years-aged concrete, amounting to about 37,50 MPa, concrete actual strength has obviously dropped in 70 years period. This may be a result of the initiation of corrosion during material durable exploitation.

The complex structural analysis performed is expected to throw more light on the character of the running processes that seriously spoiled the material strength characteristics.

2.3. Elasticity modulus of concrete

Cylindrical samples cut from the structure are used in the tests. The ratio between sample diameter and height is 1:2. Samples, together with the measuring instruments, are centered on the compression plates of a testing machine. Basic load of 0,5 N/mm^2 (MPa), **(σ_b)** is applied, held for 60 s, and displacements along each measurement line are recoded. Stresses increase gradually with constant rate until attaining a value equal to 1/3-d of the concrete cylindrical strength **($\sigma_a = f_{c,m}/3$).** The attained stress is kept constant for 60 s, while data supplied by the strain gauges are recorded along each measurement line during the first 30 s. If the difference between strains recorded along each line and the mean strain at stress σ_a is larger than 20%, new sample centering should be done.

Table 3 Modulus of elastic strains

Sample №/ Taken from block №	**σ_b, σ_a, N/mm^2**	**Δσ, N/mm^2**	**Records**			**ΔAv.**	**Δl, mm**	**Δε**	$E = \frac{\Delta\sigma}{\Delta\varepsilon}$ **N/mm^2**
			L	**R**	**Av.**				
1/blcok 2	0,5	9,5	57	45	51	28,5	0,0285	0,000285	33 300
	10		86	73	79,5				
2/block 12	0,5	9,5	42	32	37	25,5	0,0255	0,000255	37 300
	10		68	57	62,5				
3/block 19	0,5	9,5	94	64	79	29	0,0290	0,00029	32 800
	10		122	94	108				
4/block 34	0,5	9,5	88	53	70,5	26	0,0260	0,00026	36 500
	10		115	78	96.5				

Mean value E = 34 975 N/mm^2 (MPa)

At least two additional loading and unloading cycles should be realized, applying one and the same rate of stress variation and keeping constant stresses σ_a and σ_b for 60 s. After the end of the preliminary cycle and expire of the waiting period of 60 s at stress **σ_b=0,5 N/mm^2 (MPa),** strains ε_b are recorded along all deformation lines during the first 30 s. Stress increases to a value σ_a. It is then kept constant for 60 s, and records are made along all measurement lines during the first 30 s.

The static modulus of elasticity under compression is calculated on the basis of three digits using the formula:

$$E = \frac{\Delta\sigma}{\Delta\varepsilon} = \frac{\sigma_a - \sigma_b}{\varepsilon_a - \varepsilon_b}, \frac{N}{mm^2}, (MPa)$$

Test results are given in **Table 3.**

Notations:

L – record of the first (left) strain gauges;

R – record of the second (right) strain gauges;

Av. – mean record of the left and right strain gauges;

ΔAv. – difference between two successive mean records;

Δl, mm –absolute deformation of the sample (shortening of the basis of strain measurement);

The value of the secant modulus of elasticity under concrete compression seems to be plausible, and it entirely conforms to the compression strength of the tested concretes. Note also that the selected samples do not to contain visible defects (non-compacted areas and/or large air voids), which would significantly compromise concrete strength-deformation characteristics.

2.4 Water impermeability, depth of water penetration under pressure and splitting tension strength

Concrete water impermeability is the material capability to avoid water penetration when water head acts on the sample opposite sides. Impermeability of concrete depends on material type, quantity and capillary distribution within its bulk. A basic factor determining the type and volume of concrete pores is the water/cement ratio.

The coefficient of filtration of concrete is very small and oscillates within wide ranges (10^{-8}–10^{-14}) m/d. Hence, it is inconvenient for practical estimation of concrete water impermeability**.**

This impermeability is found by keeping 6 samples with diameter and height of 150 mm in water for 28 days and at temperature (20 ± 3) ºC. Testing is performed using the instrument, which enables one to subject one of the sample faces to increasing water head and examine the opposite face. The test starts under water head of 0,1 MPa, and then water pressure increases by 0,1 MPa in every 8 hours. Note that pressure should be kept constant during each 8 hours interval. When moisture appears at the opposite face of a sample prior to attaining the designed class of water impermeability, one should instantly record the respective pressure value and terminate the test. Water impermeability f a sample is taken to be the largest pressure (MPa) under which 4 out of 6 samples would not show any traces of water permeance.

When the designed class of water impermeability is attained, samples are subjected to splitting in order to find concrete tension strength. The maximal degree of water penetration (in mm) into each sample is found after splitting.

In our case however, the extraction of quality samples designed to find concrete plausible water impermeability turned out to be too difficult. This was due to the availability of non-compacted concrete areas. The results of concrete water impermeability test are generalized in **Table 4.**

Table 4 Impermeability tests results

Sample №/extracted from block №	**Pressure, MPa**	**Depth of water penetration, mm**	**Splitting tension strength, N/mm^2**
1/block 13	0,8	*	1,80
2/ block 14	0,8	25	2,20
3/ block 15	0,8	*	1,70
4/ block 16	0,8	16	2,10
5/ block 17	0,8	*	2,40
6/ block 18	0,8	20	1,50
	Mean value:	**20,30**	**1,95**

* *Water passes through the sample non-compacted areas under low pressure (0,1 MPa)*

Volume 8, ISSN 1314-7269 (Online), Published at: http://www.scientific-publications.net

The results found show that the tested concrete of well compacted areas meets the requirement of the high water impermeability lass Bв0,8, when the mean depth of water penetration under pressure of 0,8 MPa is too low- 20,3 mm**,** and the mean strength of axial tension found via splitting test is about 1,95 N/mm^2.

2.5 Depth of neutralization (carbonization) of concrete and concrete cover layer in the presence of steel reinforcement

It is proved that in the presence of oxygen and moisture, steel corrosion is initiated at environmental hydrogen factor **(**pH) lower than 11,8. The value of the hydrogen factor pH in non-damaged concrete is larger than 12,00÷12,50, which determines the high degree of environment alkalescence. Steel passivation takes place in such environment and no conditions of corrosion of the steel fiber reinforcement occur.

The high value of concrete hydrogen factor is grounded by the presence of significant quantity of calcium hydroxide **$Ca(OH_2)$** (12÷15 % of the mass of hydrated products), known also as portlandite. Yet, interacting with some components of the environment (acids, water solutions of acidic salts etc.), free lime produces salts (chlorides, sulfates, nitrates etc.) which are neutral or weakly alkaline. Hence, the hydrogen factor of concrete liquid phase drops. Below a certain level of alkalescence, a so called neutralization of concrete takes place, creating conditions of reinforcement corrosion.

On the other hand, decrease of the environment alkalescence violates also the stability of the basic hydration products that guarantees material mechanical strength and durability– calcium hydro-silicates, hydro-aluminates and hydro-ferrites. Possibility of dissociation of those compounds exists which compromises concrete strength-deformation characteristics.

Under normal exploitation and in the absence of aggressive environment, calcium hydroxide interacts with carbon dioxide in the air – a process also known as concrete carbonization. Note that environment alkalescence drops under such interaction (pH up to 8,5÷9,0). The interaction between the cement paste and carbon dioxide results in the formation of a carbonate layer. Its outside is rich of bicarbonate ions, while its inside, close to the cement particles (with high pH), consist of crystals of calcium carbonate.

The following chemical equations express carbonization:

$$\mathbf{CO_2 + H_2O = HCO_3^- \text{ (bicarbonate ion) } + H+}$$

$$\mathbf{HCO_3^- = CO_3^{2-} \text{(carbonate ion) } + H+}$$

The carbonate ion reacts with the calcium ions in the pore solution:

$$\mathbf{Ca^{2+} + CO_3^{2-} = CaCO_3}$$

This yields decrease of the concentration of calcium ions which in its turn causes dissolution of the additional quantity of calcium hydroxide (portlandite) **$Ca(OH)_2$**. Then, the following reactions take place after the exhaustion of portlandite and calcium hydro-silicates **(C-S-H),** hydro-aluminates and ettringite:

$$\mathbf{Ca(OH)_2 = Ca^{2+} + 2\ OH^- \text{ (solvability } 9{,}95 \times 10^{-4}\text{)}}$$

$$\mathbf{Ca^{2+} + CO_3^{2-} = CaCO_3 \text{ (solvability } 0{,}99 \times 10^{-8}\text{)}}$$

For pH = 9,2 (when phenol-phthalene changes its color) no calcium phase of the cement paste keeps its initial form.

Optimal conditions of the development of carbonization are available if the concrete structure is permeable and the degree of general and open porosity is large.

Consider concrete open surface and the use of pure clinker cement, type CEM I**,** in its preparation. Then, one can adopt the following tentative values of carbonization depth (mm), accounting for concrete strength (MPa) and operational conditions during a period of **t** (years) **(Table 5).**

Table 5 Carbonization depth, mm

Concrete strength, MPa	< 15 MPa	15–20 MPa	25–35 MPa	>35 MPa
Concrete in the open air, non protected	5 mm$\sqrt{t}$	2,5 mm$\sqrt{t}$	1,5 mm$\sqrt{t}$	1 mm$\sqrt{t}$

In our case, similar processes have been running for almost 70 years and concrete can be taken as non-protected and exploited in the open air. Using the above data, we can calculate the probable depth of carbonization of a tentative concrete, class B20-25. Here it amounts to 16 mm.

Hence, the process discussed so far significantly affects concrete. Considering the roof slab of the premise housing the discharge valves, advanced corrosion of its steel reinforcement is observed, together with water filtration through concrete. The development of deep corrosion in the reinforcing bars have caused decrease of steel cross-section and deterioration of steel physico-mechanical properties and bar bonding to concrete.

*2.6 Depth of concrete neutralization estimated by employing the color-metric method (conforming to standard BDS **EN14630:2007)***

The thickness of concrete neutralized area, where reinforcement bars are not corrosion-protected and products of hydration are not stable, is found by removing part of the surface concrete layer and wetting the newly formed surface with 0,1% solution of phenol-phthalene in alcohol. If the environment hydrogen factor pH is higher than 9,2, phenol-phthalene changes its color. The color of the neutralized concrete remains intact, while the non-carbonized part whose high alkalescence is kept changes its color to violet. The results found prove that the mean depth of neutralization is about 1-2 mm.

The experimentally found thickness of neutralization of the open surface of the dam wall shows that, practically, concrete carbonization has hardly taken place. This holds true for all tested control areas - even for those with non-compacted concrete. At first sight, this seems to be a paradox. Yet, it results from the very low concentration of carbon dioxide in the air, owing to dam location high above the sea level and in a protected territory with no air pollution.

2.7 Aggressive action of mild waters

Hydrate compounds forming the cement stone are more or less water-soluble. Fracture of concrete due to dissolution and extraction of components from the cement stone and concrete structure is a type of corrosion known as leaching – ***Ekström (2001)***. It is popular in East Europe and Bulgaria as **1st type corrosion** according to the classification of ***Moskvin (1980)***, or otherwise - as concrete physical corrosion.

Corrosion intensity depends in its most part on concrete permeability and type of waters washing concrete. Cement stone resistance to such impacts is determined by material composition - type of the products of hydration, as far as their water solubility is different. As in a number of cases of aggression on concrete, here the "weak point" of the phase composition of the hardened cement paste is calcium hydroxide (portlandite) formed during the interaction of the two most important clinker components-alite and belite. Their share in clinker mineral composition exceeds 75%.

In our specific case, the problem of the solubility of portlandite (the latter known as free lime) is even more serious, since free lime quantity increases with temperature decrease and increase of water purity.

Calcium hydro-silicates and hydro-aluminates, which guarantee the mechanical strength and durability of cement stone, are also pliable to dissolution. Under specific minimal concentration of **CaO** in the concrete liquid phase, they dissociate (decompose). Regarding different phases however, the minimal concentration accounted for which would guarantee stability of the hydration products varies in relatively wide range – **Table 6.**

Table 6 Limit of stability of basic clinker minerals

Cement stone mineral	Limit equilibrium concentration of CaO, g/l	
	from	to
$2CaO.SiO_2.nH_2O$	Close to the formation of saturated solution	
$3CaO.2SiO_2.nH_2O$	Close to the formation of saturated solution	
$CaO.SiO_2.nH_2O$	0,031	0,052
$4CaO.Al_2O_3.19H_2O$	1,06	1,08
$3CaO.Al_2O_3.6H_2O$	0,415	0,56
$2CaO.Al_2O_3.nH_2O$	0,16	0,36
$4CaO.Fe_2O_3.nH_2O$	over 1,06	
$2CaO.Fe_2O_3.nH_2O$	0,64	1,06
Dissociation of $Ca(OH)_2$ and $Fe(OH)_3$	under 0,64	
$3CaO.Al_2O_3.3CaSO_4.nH_2O$	under 0,045	

As said, the most hazardous effect under such impacts is water filtration through concrete. In our case, the chemical composition of dam water (stream and snow water) explicitly proves that water can be treated as mild. The value of the hydrogen factor pH varies in a narrow range (6,9-7,1), while water general hardness is about 0,42 German degrees.

Previous studies provide evidence of active filtration accompanied by the export of dissolved calcium hydroxide. Those phenomena are based on the increased value of the hydrogen factor of water in the drainage systems and on the increased water hardness. They are obviously due to the active extraction of calcium compounds from concrete during filtration.

The carbonization of concrete surface layer is of great importance for the increase of concrete stability under eventual extraction of free lime. Then, hardly soluble calcium carbide (calcite) is formed which at the same time compacts the surface layer, since volume grows by 11% during the transition $\mathbf{Ca(OH)_2 \rightarrow CaCO_3}$, and calcite solubility is $3{,}10^{-4}$g/l. Regarding the low level of carbon dioxide at high altitude, it is obvious that the phenomenon discussed is not an active protection factor.

The degree of extraction aggressiveness depends on the type of contact between the structure and water. Filtration through concrete under water head is the most dangerous process. It is assumed that the limiting factor of dissolution and extraction is diffusion of free lime from the deeper layers of the cement stone to the capillaries, cracks, pores and caverns, filtrating water. In terms of extraction, filtration through areas with local defects that have occurred during cast of concrete mix (technological joints and/or cracks) is less dangerous for the facility, as compared to the general distributed filtration through non-compacted concrete. This finding is extremely important for the concrete wall of the Beli Iskar dam. Considering that filtration runs across the concrete volume, its kinetics should be treated as dependent on the hardness of the filtrating water and on the filtration intensity. Those factors specify two possible trends of filtration development:

- Consider permeable concrete and constant water inlet (i.e. regular characteristics of hydro-technical facilities). Then, filtration will take place with non-damping rate while concrete density and subsequent strength will drop;

- If the solution of calcium hydroxide flows slowly to the open surface, precipitation of free lime in the pores of the surface concrete is possible due to water evaporation. That phenomenon often occurs when the temperature of the external surface is higher that that of the inside concrete, since lime solubility decreases. Such self-compaction of concrete is registered by a number of studies. It runs owing to the chemical interaction between cement stone phases and salts dissolved in water, and to the deposition of water-transported fine mineral particles in pores. Thus, in many cases and especially in tunnel facilities, gradual colmatation of concrete takes place, while filtration through its bulk damps in time.

Concrete manifests a capacity to self-compact in the presence of calcium or magnesium bicarbonate. It is due to the chemical interaction of free lime with compounds dissolved in water. Hence, this is one of the indexes of normalization of natural water aggressiveness. If water with high contents of carbonates filtrates through concrete, it rapidly compacts the material thus presenting no danger to the facility stability, while filtration of "hard" waters is safe only under moderate filtration flux. Unfortunately, waters in South Bulgaria and especially waters of the Beli Iskar dam, as well as rain waters, do not belong to that class. Hence, we should not expect the occurrence of concrete self-compaction during filtration.

Water hardness, resp. the value of pH in samples designed for structural analysis, is one of the basic characteristics used to identify water aggressiveness, as most normative documents state.

This marks the course of our studies in finding the value of **CaO** concentration and that of the hydrogen factor pH of samples fabricated to serve the complex structural analysis.

2.8 State of the steel reinforcement

Dam wall is built of sole concrete, while steel reinforcement is only present within the roof slab of the additional building erected in the wall middle area (the technical premise) where discharge valves are mounted. As seen, reinforcement corrosion is considerable. To reveal the reinforcement actual state we performed an instrumental control using a device for corrosion analysis **"CANIN" (Corrosion Analyzing Instrument)** manufactured by **"Proceq"** company.

We measured the electric potential (in **mV**) at different element points via a **"CANIN"** device - a copper-sulfate electrode-bar. Reinforcement potential measured on the surface of the concrete element is within limits **±900 mV** with accuracy ±3 mV conforming to the design accuracy of the instrument.

Systematic studies, including such conforming to standards ASTM C876-09 and ASTM G3-89(R10) "Standard Practice for Conventions Applicable to Electrochemical Measurements in Corrosion Testing", claim that isolated corrosion sites would be observed on the reinforcement for values larger than **200** mV, and the probability of the existence of surface corrosion is about 10%. Yet, the development of corrosion activity on the steel bar surface is questionable for values between **200** and **350 mV**, while for values higher than **350 mV** corrosion probability exceeds 90%.

Table 7 Results of the measurement of the electric-chemical potential of different steel reinforced elements

Element/position	**Electric potential between the steel reinforcement and the concrete surface, mV**									
Steel reinforced slab/technical premise	-366	-357	-392	-377	-345	-398	-404	-386	-392	-325
	-351	-358	-379	-334	-283	-320	-333	-318	-403	-423
Steel reinforced slab/technical premise	-406	-442	-433	-467	-448	-453	-455	-461	-432	-429
	-446	-437	-456	-487	-545	-518	-501	-497	-504	-545

Table 7 specifies the results found. The electric potential between the carrying steel reinforcement and the concrete surface of the analyzed slabs is higher than **350 mV.**

This fact proves that reinforcement corrosion is significant and it has spread allover the bar circumferential surface. Thus, steel-concrete bonding deteriorates, and prerequisites for concrete layer fracture arise owing to the larger volume of corrosion products. Note that corrosion is even more advanced in zones where the steel reinforcement is not protected by concrete layer.

2.9 Location, diameter and concrete covering layer of the steel reinforcement

Concrete layer thickness, as well as location and diameter of the steel reinforcement, are determined using a specialized instrument **HILTI "PS 200 Ferroscan"**. It is employed to perform operational control of the location, thickness of the concrete covering layer and diameter of the steel reinforcement via magnetic induction. The device operates in conformity with the requirements of the standard BS 1881-204:1988 "Testing concrete. Recommendations on the use of electromagnetic covermeters". Device accuracy, conforming to the

characteristics provided by the manufacturer, is ±1 mm for the diameter of the reinforcing steel and ± 3 mm for the steel distribution.

The results found for the thickness of the concrete layer covering the reinforcement are processed by means of specialized software, based on mathematical statistics and probability theory. Hence, one can perform a reliable identification of the type, diameter and location of the steel reinforcement.

3. COMPLEX STRUCTURAL ANALYSIS PERFORMED TO IDENTIFY POTENTIAL CORROSION PROCESSES AND THEIR EFFECT ON HYDRATION PRODUCTS

3.1 Sampling

Cores were extracted to assess the strength-deformation characteristics of concrete (blocks №№ 8, 10, 11, 18, 21, 28 and 34).

Prior to core testing, samples were taken from some of them (**at three different depths (0-2 cm, 2-5 cm and 5-8 cm).** They were analyzed using various structural methods, i.e. chemical-analytical method to find the concentration of **CaO** and the hydrogen index pH, X-ray phase analysis **(**XRPA**),** differential thermal analysis (DTA), mercury porometry (MP) and scanning electronic microscopy (SEM).

3.2 CaO concentration and pH-value

As discussed, the stable presence of the basic hydration products in the cement stone is directly related to the specific level of **CaO** concentration, (to pH of the environment, respectively), and those levels determine system stability. In particular, they affect the eventual occurrence of crystal decomposition yielding violation of concrete strength-deformation characteristics. Under the effect of the environmental factors already discussed (filtration of “mild” waters, cyclic water saturation and drying, freezing-unfreezing, solar radiation, partial carbonization) evidence of **CaO** concentration and pH is expected to be very informative. It could be especially useful to correctly interpret data acquired via other methods of analysis considered in the investigation program.

We use methods of the analytical chemistry to identify the material characteristics. **Table 8** specifies the results of sample testing**.**

Table 8 Concentration of calcium oxide and value of the pH index

Sample	**Studied characteristics**	
№	**CaO, g/l**	**pH**
1	0,42	12,04
2	0,56	12,06
3	0,62	12,20
4	0,31	11,88
5	0,43	12,06
6	0,48	12,13
7	0,58	12,05
8	0,69	12,12
9	0,72	12,18
10	0,25	11,98
11	0,44	12,03
12	0,57	12,06
13	0,15	11,51

14	0,20	11,60
15	0,31	11,82
16	0,36	11,95
17	0,44	12,01
18	0,59	12,04
19	0,22	11,84
20	0,26	11,91
21	0,44	11,96

The hydrogen factor pH is identified employing the potential-measurement method in analyzing the suspension remaining after filtering.

The results for the pH factor show that the alkalinity of the environment has been kept to a large extent within the concrete samples, including those taken from the concrete surface.

As for the specific concentration of **CaO,** its values are bound to special analysis, comparing them to the limit values of stable existence of the hydration basic products, as given in **Table 6**. It is seen that the levels of **CaO** in the samples are lower than those guaranteeing solution saturation (about 1,25 g/l), while some of them are below the stability critical levels of some basic hydro-silicates, hydro-aluminates and hydro-ferrites. This evidence needs additional interpretation via other methods of complex structural analysis.

3.3 X-ray-phase analysis

The X-ray analysis is a universal method of studying crystal silicate materials. Thus, one can perform quantitative and qualitative analysis of materials with complex composition, measure crystal dimensions, assess internal stresses, follow synthesis and decomposition of compounds etc.

The results found in our study are graphically presented by “stacking” the X-ray grams recorded for each three samples extracted at various depths from one and the same core (**Fig. 1**).

Thus, the eventual difference between the peaks, corresponding to the basic compounds identified at the three levels of investigation, is visualized, and one can directly assess corrosion processes having run at each discrete depth. The identification of the basic hydro-compounds within the studied samples is presented in the respective X-ray grams.

The analysis of the results found leads to the following conclusions of major importance:

An almost entire overlay of the basic peaks of the recorded X-ray grams is seen. This finding confirms the usage of identical type of cement in the wall construction, and one can be more confident in interpreting the results of the structural investigation.

No serious instability and dissociation of the basic hydration products, that would seriously violate the basic strength-deformation characteristics of concrete, were established.

Approaching the concrete/air interface, the quantity of portlandite in the hardened concrete decreases. This seems logical. Yet, under decreased **CaO** concentration within the system, the absence of high-basic calcium hydro-silicates is embarrassing, as far as those compounds are in direct relation with concrete strength-deformation characteristics.

On one hand, this can be explained with the crystal finely-dispersed polymerization (gel-formation) having taken place, but on the other hand, it could be an indication of crystal partial decomposition under shortage of **CaO** in the environment**.**

3.4 Differential-thermal analysis

The differential-thermal analysis (DTA) enables one to find whether phase transformation proceeds or do not take place during heating of the studied compound.

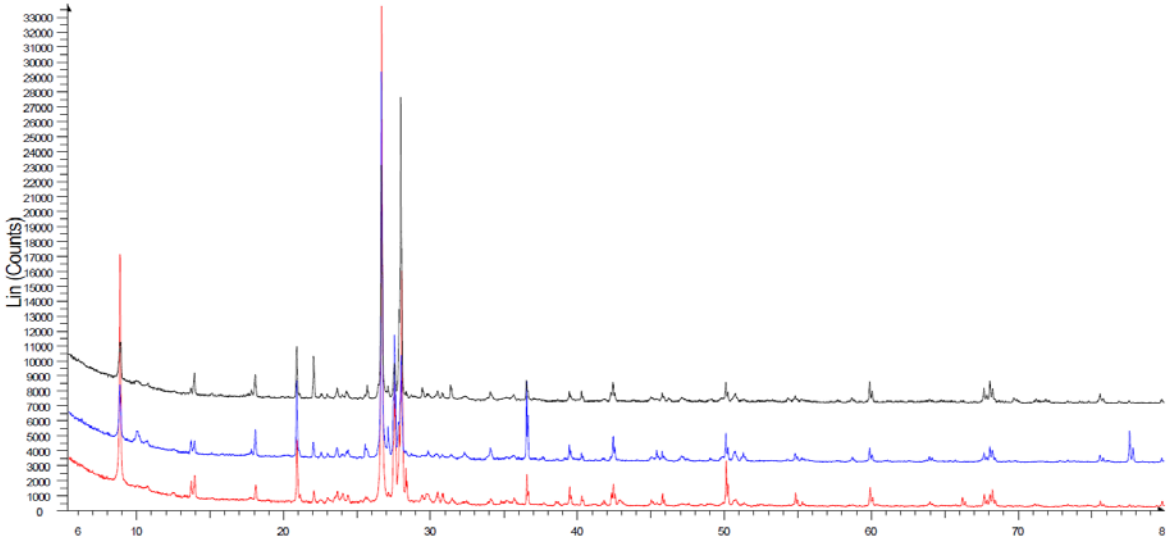

Fig. 1 XRD – samples 0, 2 and 8 cm in cross-section depth

The researcher can also find the rate of the running chemical reactions or phase transformations, or assess the quantity of compounds participating in the reactions. The identification of the basic endo-effects, and respectively, the identification of the characteristic hydro-compounds within the analyzed samples, are presented in **Table 9** and shown in **Figures 2, 3** and **4.**

The following conclusions follow from the above considerations: The thermo-grams illustrate some characteristic endo-thermal effects. The latter are linked with dehydration and decomposition of a number of hydration products: (i) calcium hydro-silicates, calcium hydro-aluminates and ettringite (with dehydration temperature about 450-500 ^{0}C, i.e. so called products with low dehydration temperature); (ii) products, including calcite, with dehydration temperature higher than 750-850 ^{0}C **(**products with high dehydration temperature).

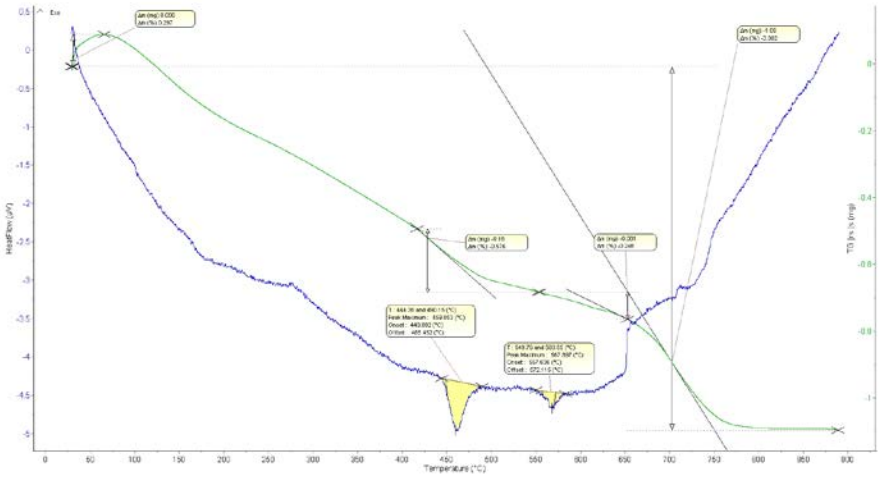

Fig. 2 Sample extracted at 0-2 cm depth

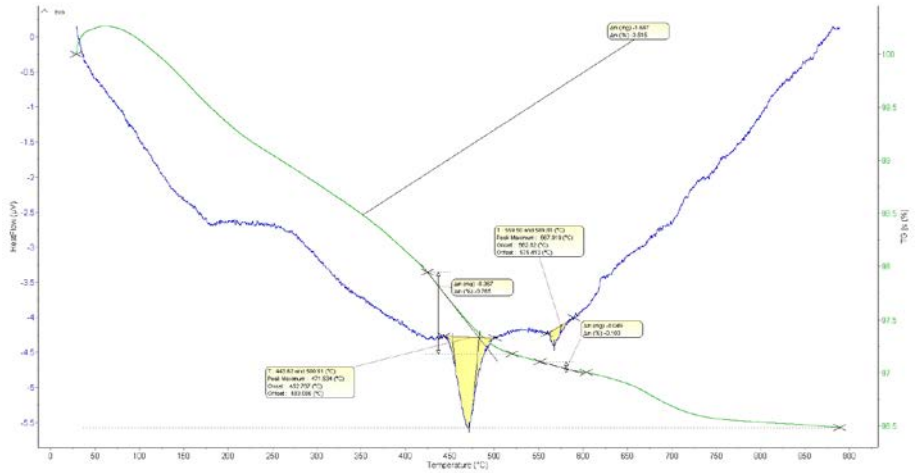

Fig. 3 Sample extracted at 2-5 cm depth

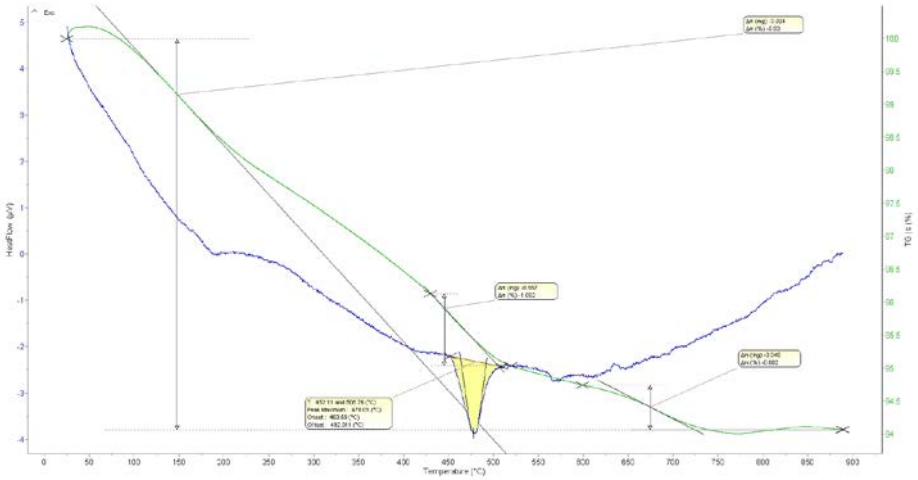

Fig. 4 Sample extracted at 5-8 cm depth

A characteristic peak of portlandite is also observed (within the range 530-580 ^{0}C).

Evaporation of crystal-bonded water from the structure of calcium hydro-silicates and hydro-aluminates is not observed within the temperature range of 350–400 ^{0}C. Principally, this phenomenon can be treated as an integral indication that no decomposition runs under the action of "mild" waters, owing to the high degree of polymerization (gel formation) observed in such compounds of 4-5 years age.

On the other hand, however, comparing those results to the lower **CaO** concentration in all samples, the lack of evaporation can be considered as an indication of partial dissociation of those compounds, which would integrally deteriorate concrete strength-deformation characteristics.

As found using the phenol-phthalene method of analysis, the presence of portlandite in all samples verifies the high value of pH and the alkaline reaction of the hardened concrete.

Table 9 Generalized DTA data

Sample	**Compound/ Loss of mass within the temperature range (^{0}C), %**			
№	**nC-S-H$_i$ 450-500**	**Portlandite 530-580**	**Calcite 750-850**	**Total loss 20-900**
1	0,576	0,246	-	3,302
2	0,765	0,103	-	3,515
3	1,092	0,682	-	5,930
4	0,338	2,96	-	7,289
5	0,931	0,945	-	6,488
6	0,853	-	-	4,708
7	0,637	1,245	-	4,464
8	0,796	-	0,267	4,900
9	0,813	-	-	5,642
10	0,458	0,085	1,739	5,188
11	0,630	0,864	-	5,062
12	0,751	0,806	-	4,403
13	0,179	следи	-	1,449
14	0,233	0,071	0,372	4,413
15	0,471	0,122	-	0,822
16	0,314	0,103	1,325	5,418
17	0,336	0,082	0,565	3,946
18	0,380	0,091	0,629	4,071
19	1,345	0,051	2,833	9,723
20	1,186	-	0,907	5,188
21	0,617	0,061	0,672	3,462

Deposits on the wall surface, being products of water filtration and portlandite extraction from the structure of the hardened concrete, consist of calcium carbonate (lime stone, calcite).

3.5 Scanning electron microcopy

Using an electron microscope to examine binders, one can study important properties of separate sub-micro crystals, such as shape and dimensions, as well as crystal growth and fracture occurring either in the solution or in the solid phase.

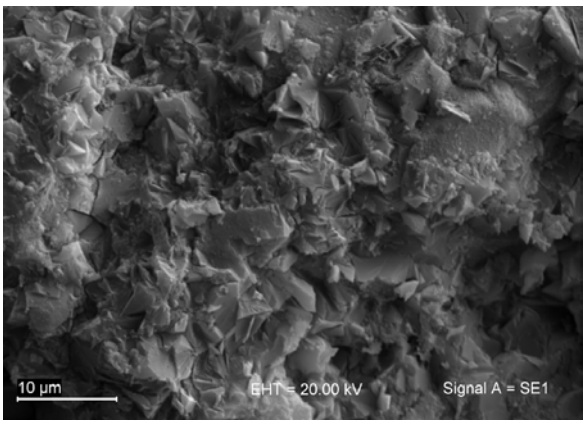

Photo 1

Sample extracted at 0-2 cm depth

Concrete samples are taken at various depths (0-2 cm, 2-5 cm и 5-8 cm) - **Photo 1**. They are dried in a vacuum drier to a constant mass, processed with gold powder to get a better image contrast and then inspected using a scanning electron microscope with different resolution and magnification.

All photos show the availability of lighter crystals of calcite (calcium carbonate) with different shape and dimensions and darker crystals of calcium hydro-silicates.

The general tendency is in-depth decrease of calcite amount, which can be explained with the hard access of carbon dioxide initiating concrete carbonization and calcite formation.

As for calcium hydro-silicates **(C-S-H)** determining concrete strength-deformation characteristics, such tendency is not observed – they are almost identical at the three studied depths.

Together with the products of hydration, the photos show also a number of pores and cracks as fixed elements of concrete structure. Photos of deposits on the concrete surface show that they are mostly calcium carbonates, as confirmed by other methods of structural study.

3.6 Mercury porometry

The method of mercury porometry is based on the phenomenon that a liquid, not wetting a solid body, penetrates its pores due to external pressure, only. The volume of the filling liquid is a function of the external pressure, and on that basis, one can get information on the pore distribution with respect to dimensions.

The results found yield the following conclusions:

The obtained integral and differential curves of pore distribution with respect to dimensions are typical for concrete of advanced age. The volume of micropores **(**with radius of up to 0,05µm) is significantly reduced, due to hydration that causes pore filling with hydration products. At the same time, the share of pores larger than 1000 ηm is significant– over 65% (to 90 %), since chemical products can hardly fill them.

The significant volume of macropores illustrates the insufficient compaction of the structure, resulting in increase of concrete permeability and initiation of corrosion damage.

Despite the large amount of experimental evidence, we can not find an in-depth tendency of modification of the concrete pore relative volume and pore space character. This fact once again confirms our conclusion that concrete compaction is non-uniform within different sections.

3.7 Generalized results of the structural studies

Complex structural studies have been performed, including determination the of **CaO** concentration in the system, specification of the hydrogen factor pH and identification of the basic hydration compounds of the concrete cement stone and parameters of the pore structure. Hence, plausible conclusions on the internal structural state of concrete can be drawn, considering a long period of exploitation under active atmospheric and corrosion impacts:

The values of the hydrogen factor pH show that material alkelscence within the samples has been kept constant to a large extent, including samples extracted from the concrete surface. As for the **CaO** concentration, it is seen that its values are lower than the critical value of the solution saturation (about 1,25 g/l), while some of them are lower than the critical values of stability of some basic hydro-silicates, hydro-aluminates and hydro-ferrites.

An almost entire overlap of the basic peaks is seen in the X-ray graphs, confirming that identical type of cement has been used during the whole construction period.

No serious instability and dissociation of the basic hydration products have been identified to yield violation of the basic strength-deformation characteristics of concrete. Yet, the lack of basic newly formed hydration products indicates initiation of such a process, which is definitely embarrassing.

It seems reasonable that the quantity of portlandite in concrete decreases when approaching the concrete/air interface.

The plotted integral and differential curves of pore distribution with respect to dimensions are typical for concrete of advanced age. The volume of micro-pores (with radius of up to 0,05μm) is significantly reduced, due to the duration of hydration, when volume of pores decreases as a result of pore filling with newly formed hydration products. At the same time, the share of pores exceeding 1000 ηm is significant – over 65% (to 90 %), since they can be hardly filled. The significant volume of macropores proves the insufficient compactness of the concrete structure. In its turn, the non-compacted structure favors an in-depth invasion of various chemical agents, rain water and carbon dioxide in particular, yielding corrosion of the cement stone and concrete.

Despite the significant experimental evidence, we could not establish a specific tendency оf variation of pore relative volume and space character– in depth or within different concrete wall sections. This additionally proves our deduction that concrete compaction is non-homogeneous.

4. BASIC CONCLUSIONS AND RECOMMENDATIONS

The analysis of our results allows for the formulation of specific **BASIC CONCLUSIONS** concerning the state of concrete, namely:

70 years back, the technological level of building had a direct effect on the integral characteristics of the wall concrete. A number of problems were uncovered, mostly related to the inhomogeneous compaction of the concrete mix and the technology of arrangement and processing of the work joints. This resulted in non-homogeneity of concrete strength-deformation characteristics, as found in our study, hampering the identification of specific areas (separate blocks, for instance) with approximately identical characteristics.

Since the time of wall construction, concrete has been exploited under the action of active environmental factors, including “mild” waters filling the dam cup and causing corrosion. Despite the numerous measures of wall repair and rehabilitation, filtration of mild waters through the work joints and wall has proceeded to inflict wall corrosion, as established some years ago.

The recently identified strength-deformation characteristics of concrete satisfactorily meet the prescribe requirements, but they reflect the state of concrete in areas relatively uniform, well compacted and non-damaged. Yet, this is not the case of areas of active leaching and intensive development of corrosion, which the safety of the entire facility depends upon.

Based on the complex structural analysis, we may reliably claim that the exploitation environment gradually extends the in-depth development of concrete corrosion mostly expressed in the “export” (extraction) of calcium hydroxide through concrete connected pores. That activity specifies the kinetics of gradual decrease of the level of calcium oxide. The phenomenon is closely related to the stable existence of basic hydro-compounds in the cement stone that form the strength-deformation characteristics of concrete.

We have established active corrosion of the reinforcing steel in the areas of concrete reinforcement (the technical premises), endangering structure safety.

Based on the above considerations, we can set forth some specific **RECOMMENDATIONS** to keep and guarantee concrete strength-deformation characteristics, which determine facility safe exploitation:

It is of crucial importance to develop an investment operational project for wall rehabilitation, which should include **at least two basic actions**:

Undertake of specialized measures (rehabilitation of the geo-membrane at the water/wall interface, preparation of injection curtains, elimination of the eventual inflow of slope waters soaking the wall concrete body etc.) that would block filtration and increase the impermeability of the entire concrete cross section, especially in the areas where vertical and horizontal joints have been shaped;

Development of a technological system to heal the concrete surface. It should provide: localization of the areas of concrete corrosive and mechanical damage; appropriate removal of the damaged concrete (mechanically, via sand jetting, hydro-blasting etc.) and reaching a solid base; processing and compaction of joints between separate wall sections; cross section rehabilitation using an appropriate repair materials; deposition of a secondary finishing layer on the concrete surface to protect it from atmospheric impacts; fabrication of hydro-insulation, processing of the corroded steel bar reinforcement and rehabilitation of the concrete cross section of the roof of premises housing water discharging valves.

REFERENCES

ICOLD Committee on Concrete Dams. The Physical Properties of Hardened Conventional Concrete, March, 2008.

International Commission on Large Dams, The Specification and Quality Control of Concrete Dams, Bulletin 136, 2009, No24992, ISSN 0534-8293.

Ekström T. Leaching of Concrete, Experiments and Modeling, Lund Institute of Econology, Report RVBM 3090, 2001.

Москвин В. М., Ф. М. Иванов, С.Н. Алексеев, Е. А. Гузеев. Коррозия бетона и железобетона, методы их защиты. Москва, Стройиздат, 1980, УДК 691.32:020.193/197.